JCTC Journal of Chemical Theory and Computation

Article

pubs.acs.org/JCTC

A Green's-Function Approach to Exchange Spin Coupling As a New Tool for Quantum Chemistry

Torben Steenbock,[†] Jos Tasche,[‡] Alexander I. Lichtenstein,[§] and Carmen Herrmann*[,†]

[†]Department of Chemistry, University of Hamburg, Hamburg, Germany

[‡]Department of Chemistry, Durham University, Durham, United Kingdom

[§]Department of Physics, University of Hamburg, Hamburg, Germany

Supporting Information

ABSTRACT: Exchange spin coupling is usually evaluated in quantum chemistry from the energy difference between a high-spin determinant and a Broken-Symmetry (BS) determinant in combination with Kohn−Sham density functional theory (KS-DFT), based on the work of Noodleman. As an alternative, an efficient approximate approach relying on Green's functions has been developed by one of the authors. This approach stems from solid-state physics and has never been systematically tested for molecular systems. We rederive a version of the Green's-function approach originally suggested by Han, Ozaki, and Yu. This new derivation employs local projection operators as common in quantum chemistry for defining local properties such as partial charges, rather than using a dual basis as in the Han−Ozaki−Yu approach. The result is a simple postprocessing procedure for KS-DFT calculations, which in contrast to the BS energy-difference approach requires the electronic structure of only one spin state. We show for several representative small molecules, diradicals, and dinuclear transition metal complexes that this method gives qualitatively consistent results with the BS energy-difference approach as long as it is applied to high-spin determinants and as long as structural relaxation effects in different spin states do not play an important role.

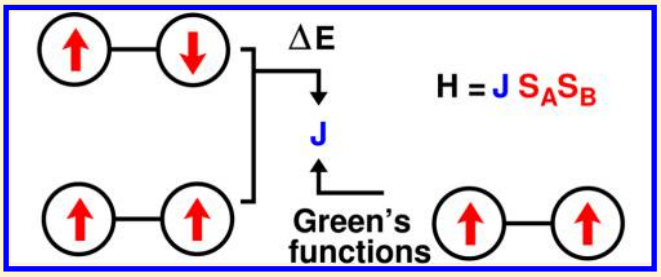

1. INTRODUCTION

Exchange coupling between electron spins is important in many compounds, especially in polynuclear transition metal complexes with partially filled d orbitals[1,2] and in organic polyradicals.[3] In addition to direct exchange coupling between two metal centers, it is possible that closed-shell bridging ligands between two metal centers mediate the coupling. This is referred to as super-exchange.[4,5] Exchange-coupled molecular compounds are candidates for molecular spintronics[6,7] and are extensively studied in the field of molecular magnetism.[2] Spin coupling is also important in biological systems, in particular in active sites of enzymes such as methane monooxygenase, which contains a di-μ-oxo-diiron core exhibiting magnetic coupling between the iron centers via the oxo ligand.[8,9] Spin coupling is equally relevant for a range of synthetic homogeneous catalysts.[10,11] It can be regarded as an example of a more general phenomenon, communication through molecular bridges.[12−14]

Experimentally, the nature (ferromagnetic vs antiferromagnetic) and strength of exchange coupling is usually determined from the temperature dependence of the magnetic susceptibility. The resulting curves are fitted to a spin Hamiltonian (see eq 1 below), resulting in an exchange spin coupling constant J.[15−20] Sometimes an unambiguous fit is not possible experimentally, so theoretical calculations are a very valuable complement to experiments. Furthermore, such calculations offer a more detailed understanding of chemical mechanisms behind spin coupling and can help to design new compounds with desired magnetic properties. Due to the typical size of the systems under study, Kohn−Sham density functional theory (KS-DFT)[21] is by far the most popular electronic structure method in this context. In 1981, Noodleman derived the so-called Broken-Symmetry (BS) formalism, which enables the calculation of J from the energy difference between the high-spin and a so-called BS determinant[22] by applying spin projection. The BS determinant describes the antiferromagnetically coupled state as having local spins with the same magnitudes, but opposite signs on both magnetic sites (for a system with two identical spin centers). Although this description introduces an artificial spin density which is not present in a real singlet state, it has been successfully applied to a variety of systems.[8,23−27] Noodleman's approach may be considered today's standard method for evaluating exchange coupling constants in quantum chemistry.

Another approach for calculating J based on Green's functions comes from solid-state physics. It was first published by one of the authors in 1984 for the description of Ruderman−Kittel−Kasuya−Yoshida (RKKY) coupling of impurity atoms in metals[28]. It was derived by comparing the energy change due to a small rotation of a local spin vector between a Green's-function energy expression and the Heisenberg model,[29] using the local force theorem. Han et al. have implemented a version of this approach in the program OpenMX,[30] where it can be used in

Received: April 14, 2015
Published: October 27, 2015

ACS Publications © 2015 American Chemical Society

DOI: 10.1021/acs.jctc.5b00349
J. Chem. Theory Comput. 2015, 11, 5651−5664

combination with unrestricted KS-DFT.[31] This version is conceptually interesting since it can be written as the sum of contributions from pairs of molecular orbitals occupied by electrons of opposing spins. This suggests using this method as a tool for understanding magnetic coupling in terms of exchange pathways.[25,32]

A conceptually related approach has been published by Peralta and co-workers,[33,34] in which all magnetic exchange couplings of a molecule are calculated from derivatives of the energy with respect to spin rotations in the high-spin configuration based on a perturbative approach within non-collinear density functional theory. It was applied to various transition-metal complexes, and the obtained magnetic exchange coupling constants are in a very good agreement with Noodleman's Broken-Symmetry approach. While this approach employs an iterative coupled-perturbed Kohn–Sham scheme, the Green's-function approach employed here is a simple postprocessing tool (possibly at the cost of reduced accuracy).

While the Green's-function approach has been used to describe atomic adsorbates on surfaces[35,36] and magnetic solids,[37−39] applications to molecules are rare and, to the best of our knowledge, include manganese and vanadium complexes only.[31,40] Therefore, our goal is to check systematically if the Green's function approach gives reliable results compared with Noodleman's approach for chemically relevant compounds. Note that our reference is not the experiment, but DFT in combination with the Broken-Symmetry approach: If DFT+BS fails to reproduce the measured spin coupling (either because of methodological shortcomings or because of neglected intermolecular interactions), the Green's-functional approach should fail in the same way.

We first review the theoretical background briefly in section 2 and then rederive the Han–Ozaki–Yu version of the Green's function approach using local projection operators as frequently used in population analysis and other local partitioning methods in quantum chemistry[41] in section 3. We have implemented the resulting equation in our tool for postprocessing electronic-structure calculations, Artaios,[42] and apply it to a series of molecular structures in the following sections. In this initial study, we define the spin center as the formally spin-carrying atom only rather than including ligand atoms on which the spin may be delocalized, to check whether this simple approach allows for qualitative accuracy. First, we study simple model systems for exchange and superexchange, H_2 and H–He–H, which we use to evaluate the importance of the choice of exchange–correlation functional and basis set (section 5). Then, we investigate several dinuclear transition metal complexes and *para*- and *meta*-connected dimethylbenzene radicals, which we group according to whether the spin density is mainly localized on the formally spin-carrying atoms (section 6) or not (section 7). Here, we also discuss the importance of structural relaxation in the different spin states. In section 8, we finally evaluate qualitative trends as a function of bridging angle for systems with delocalized spins, dinuclear hydroxo-bridged copper(II) complexes as investigated by Hoffmann and co-workers.[1] Our findings are summarized in section 9.

2. THEORETICAL BACKGROUND

2.1. The Heisenberg Hamiltonian. The Heisenberg–Dirac–van Vleck (HDvV) Hamiltonian is an effective Hamiltonian which describes magnetic exchange coupling in chemical compounds and solids and is formulated as the sum over pairs of spin centers *A*, *B*, ...

$$\begin{aligned}\hat{H}_{\mathrm{HDvV}} &= -2\sum_{A<B} J_{AB}\hat{\mathbf{S}}_A\hat{\mathbf{S}}_B \\ &= -2\sum_{A<B} J_{AB}S_AS_B\hat{\mathbf{e}}_A\hat{\mathbf{e}}_B \\ &= -2\sum_{A<B} J_{AB}S_AS_B\cos(\theta_{AB})\end{aligned} \tag{1}$$

where J_{AB} are the coupling constants and $\hat{\mathbf{S}}_A$ and $\hat{\mathbf{S}}_B$ are local spin vectors on different atoms *A* and *B*. In eq 1, the local spin vectors can be decomposed into the magnitude S_A and a vector of unit length $\hat{\mathbf{e}}_A$ describing the spin orientation. The product of these unit vectors is equal to the cosine of the angle between the spin vectors on both spin centers, θ_{AB}. The spin centers can be, in principle, atoms or groups of atoms, but in the following, we always choose one atom. J_{AB} is positive for ferromagnetic coupled spins (parallel alignment) and negative for antiferromagnetically coupled ones (antiparallel alignment).

Equation 1 for the Heisenberg–Dirac–Van Vleck Hamiltonian is only valid for insulators and semiconductors where the spin is localized.[28,43] For metals, a Hamiltonian containing spin operators $\hat{\mathbf{e}}_A$ with unit length is employed instead:[28,43,44]

$$\hat{H}^{\mathrm{Unit}}_{\mathrm{HDvV}} = -\sum_{A<B} 2J^{\mathrm{unit}}_{AB}\hat{\mathbf{e}}_A\hat{\mathbf{e}}_B \tag{2}$$

The local spin operator $\mathbf{S}_A$ can be obtained by multiplication of $\hat{\mathbf{e}}_A$ by the local spin vector length $S_A = |\mathbf{S}_A|$ (e.g., $S_A = 1/2$ for one unpaired electron on *A*):

$$\hat{\mathbf{S}}_A = S_A\hat{\mathbf{e}}_A \tag{3}$$

This form of the Hamiltonian is later used in the derivation of the expression used in the Green's-function approach. The coupling constants for two cases are thus related by

$$J_{AB} = \frac{J^{\mathrm{unit}}_{AB}}{S_AS_B} \tag{4}$$

In the following, we assume ideal local spin vectors; that is, S_A is one-half the number of formally unpaired electrons on *A* (which may in practice be diminished by spin delocalization).

2.2. Noodleman's Broken-Symmetry Approach to Spin Coupling. In quantum chemistry, usually a method proposed by Noodleman is employed,[22] in which the coupling constant is calculated based on spin projection for two spin centers from the energy difference between the high-spin or ferromagnetically coupled (F) and the Broken-Symmetry (BS) determinants:

$$J_{\mathrm{BS,projected}} = -\frac{E^{\mathrm{F}} - E^{\mathrm{BS}}}{S^2_{\mathrm{F}}} \tag{5}$$

The subscript *AB* was omitted here and in the following for better readability. S_{F} is the total spin quantum number in the ferromagnetic state. The BS determinant is an approximation to the low-spin state, which cannot be described accurately within one-determinental methods as KS-DFT. In the case of a singlet low-spin state in a diradical, the BS determinant is an equal admixture of triplet and singlet, with α (or spin-up or majority) spin density on one and β (or spin-down or minority) spin density on the other spin center. The energy of the singlet state is extracted by applying projection operators. It is debatable whether this spin projection is needed in a KS-DFT framework.[45,46] Therefore, we will compare with coupling constants which assume that the BS determinant gives the correct energy of the singlet:

DOI: 10.1021/acs.jctc.5b00349
J. Chem. Theory Comput. 2015, 11, 5651−5664

$$J_{\mathrm{BS,unprojected}} = -\frac{E^{\mathrm{F}} - E^{\mathrm{BS}}}{S_{\mathrm{F}}(S_{\mathrm{F}}+1)} \tag{6}$$

From now on, we will refer to eq 5 as the projected Noodleman equation and to eq 6 as the unprojected Noodleman equation.

2.3. Green's-Function Approach. An alternative ansatz for the evaluation of magnetic exchange coupling constants was derived by one of the authors by comparing the energy change due to a small spin rotation between a Green's-function energy expression and the Heisenberg model,[29] using the local force theorem. The energy is assumed to have a cosine dependence on the relative angle between the local spins, and since in this case the energy splitting between ferro- and antiferromagnetically coupled states can be obtained from the second derivative of the energy with respect to rotation of one spin vector, the electronic structure of only one spin state needs to be known. The final expression for the Heisenberg exchange coupling constant $J^{\mathrm{unit}}_{\mathrm{Green}}(\mathrm{F})$ for local spin vectors of unit length (eq 2) calculated from the ferromagnetically (F) coupled state is obtained as the imaginary part of an integral over the trace of products of the Green's functions for α and β spins and so-called on-site potentials $\hat{V}_A$ and $\hat{V}_B$ of the two magnetic sites:

$$J^{\mathrm{unit}}_{\mathrm{Green}}(\mathrm{F}) = -\frac{1}{4\pi} Im \int_{-\infty}^{\epsilon_{\mathrm{F}}} \mathrm{d}\epsilon\, Tr[\hat{V}_A \hat{G}^{\alpha} \hat{V}_B \hat{G}^{\beta}] \tag{7}$$

The on-site potentials can be expressed as the difference between the Coulomb potentials for α and β electrons, $\hat{U}^{\alpha}_A$ and $\hat{U}^{\beta}_A$:

$$\hat{V}_A = \hat{U}^{\alpha}_A - \hat{U}^{\beta}_A \tag{8}$$

2.4. Local Spins. When using the Heisenberg Hamiltonian, one assumes that the magnitude of local spins is the same in different spin states. This is an assumption that needs to be checked in KS-DFT calculations. Therefore, often a local spin analysis is carried out which gives the local contributions $\langle \hat{S}_{zA} \rangle$ from an atom or fragment A to the expectation value of the z component of the total spin operator, $\hat{S}_z$. $\langle \hat{S}_{zA} \rangle$ can be calculated as one-half the difference of the local populations of α and β electrons, N^{α}_A and N^{β}_A, as

$$\langle \hat{S}_{zA} \rangle = \frac{1}{2}(N^{\alpha}_A - N^{\beta}_A) \tag{9}$$

This equation provides a connection between the local spins and the population analysis. The first schemes for the population analysis were derived by Löwdin[47] and Mulliken.[48] In this work, we have only used the latter, as the local partitioning scheme has been shown to have little influence on local spins (in contrast to population analysis).[49] Within the Mulliken local partitioning scheme, the number of electrons on a center A is calculated from matrix elements of the product of the density matrix $\mathbf{P}$ for α and β electrons, respectively, and the elements of the overlap matrix $\mathbf{S}$ between pairs of atom-centered basis functions μ and ν:[50]

$$N^{\sigma}_A = \sum_{\mu \in A} (\mathbf{P}^{\sigma}\mathbf{S})_{\mu\mu} \tag{10}$$

with $\sigma \in \{\alpha,\beta\}$.

3. THE GREEN'S-FUNCTION APPROACH IN TERMS OF LOCAL PROJECTION OPERATORS

In the following, we rederive the Han–Ozaki–Yu version of eq 7[31] employing local projection operators. This allows for employing different local partitioning schemes available in quantum chemistry to be used for the definition of the on-site potentials.

Equation 7 can be reformulated by considering that $Im(AB) = Im(A)\, Re(B) + Re(A)\, Im(B)$:

$$J^{\mathrm{unit}}_{\mathrm{Green}}(\mathrm{F}) = -\frac{1}{4\pi} \int_{-\infty}^{\epsilon_{\mathrm{F}}} \mathrm{d}\epsilon\, Tr[\hat{V}_A Im(\hat{G}^{\alpha}) \hat{V}_B Re(\hat{G}^{\beta}) + \hat{V}_A\, Re(\hat{G}^{\alpha}) \hat{V}_B\, Im(\hat{G}^{\beta})] \tag{11}$$

The Green's functions are expressed in a Kohn–Sham molecular orbital (MO) basis $\{|\phi^{\sigma}_i\rangle\}$ by using the definition:

$$\hat{G}^{\sigma}(\epsilon) = \lim_{\delta \to 0+} (\epsilon - \hat{h}^{\sigma} + i\delta)^{-1} \tag{12}$$

where the effective single-particle (or, here, Kohn–Sham) Hamiltonian in the basis of molecular orbitals is

$$\hat{h}^{\sigma} = \sum_i |\phi^{\sigma}_i\rangle \epsilon^{\sigma}_i \langle \phi^{\sigma}_i| \tag{13}$$

and where ϵ^{σ}_i refers to the energy of MO $|\phi^{\sigma}_i\rangle$ with spin $\sigma \in \{\alpha,\beta\}$. We insert eq 13 into eq 12 to obtain the final expressions for the Green's functions in the Kohn–Sham orbital basis:

$$\hat{G}^{\sigma}(\epsilon) = \sum_i \frac{|\phi^{\sigma}_i\rangle\langle\phi^{\sigma}_i|}{\epsilon - \epsilon^{\sigma}_i + i\delta} \tag{14}$$

Within an integral, the denominator of eq 14 can be rewritten as

$$\frac{1}{\epsilon - \epsilon^{\sigma}_i + i\delta} = P\frac{1}{\epsilon - \epsilon^{\sigma}_i} - i\pi\delta(\epsilon - \epsilon^{\sigma}_i) \tag{15}$$

where P refers to the Cauchy principal part. According to eq 15, the imaginary and real parts of the Green's function are given as

$$Im(\hat{G}^{\sigma}) = -\pi \sum_i |\phi^{\sigma}_i\rangle\langle\phi^{\sigma}_i|\delta(\epsilon - \epsilon^{\sigma}_i) \tag{16}$$

$$Re(\hat{G}^{\sigma}) = \sum_i \frac{|\phi^{\sigma}_i\rangle\langle\phi^{\sigma}_i|}{\epsilon - \epsilon^{\sigma}_i} \tag{17}$$

By inserting eqs 16 and 17 into eq 11, we obtain

$$J^{\mathrm{unit}}_{\mathrm{Green}}(\mathrm{F}) = -\frac{1}{4} \int^{\epsilon_{\mathrm{F}}} \mathrm{d}\epsilon\, Tr[\sum_{i,j} \hat{V}_A |\phi^{\alpha}_i\rangle\langle\phi^{\alpha}_i|\delta(\epsilon - \epsilon^{\alpha}_i) \hat{V}_B \frac{|\phi^{\beta}_j\rangle\langle\phi^{\beta}_j|}{\epsilon - \epsilon^{\beta}_j} + \hat{V}_A \frac{|\phi^{\alpha}_i\rangle\langle\phi^{\alpha}_i|}{\epsilon - \epsilon^{\alpha}_i} \hat{V}_B |\phi^{\beta}_j\rangle\langle\phi^{\beta}_j|\delta (\epsilon - \epsilon^{\beta}_j)] \tag{18}$$

Employing the properties of the Dirac function:

$$\int_{-\infty}^{\infty} \mathrm{d}\epsilon\, f(\epsilon)\, \delta(\epsilon - \epsilon^{\sigma}_i) = f(\epsilon^{\sigma}_i) \tag{19}$$

we obtain

$$J^{\mathrm{unit}}_{\mathrm{Green}}(\mathrm{F}) = -\frac{1}{4} Tr\left[\sum_{i \in \mathrm{occ},j} \hat{V}_A |\phi^{\alpha}_i\rangle\langle\phi^{\alpha}_i| \hat{V}_B \frac{|\phi^{\beta}_j\rangle\langle\phi^{\beta}_j|}{\epsilon^{\alpha}_i - \epsilon^{\beta}_j} + \sum_{j \in \mathrm{occ},i} \hat{V}_A \frac{|\phi^{\alpha}_i\rangle\langle\phi^{\alpha}_i|}{\epsilon^{\beta}_j - \epsilon^{\alpha}_i} \hat{V}_B |\phi^{\beta}_j\rangle\langle\phi^{\beta}_j| \right] \tag{20}$$

The two terms appearing in eq 20 differ in the order of the molecular orbital energy differences. Since the Fermi energy

DOI: 10.1021/acs.jctc.5b00349
J. Chem. Theory Comput. 2015, 11, 5651–5664

constitutes the upper bond of integration, the sums are restricted to occupied α spin−orbitals in the first term and to occupied β spin orbitals in the second term.

The on-site potentials can be defined with local projection operators $\hat{p}_A$, which we choose in the following according to Löwdin's partitioning scheme:

$$\hat{p}_A = \sum_{\mu \in A} |\mu\rangle\langle\mu| \tag{21}$$

where the $|\mu\rangle$'s are symmetrically orthogonalized atom-centered one-particle basis functions, resulting in

$$\hat{V}_A = \hat{p}_A(\hat{h}^\alpha - \hat{h}^\beta)\hat{p}_A = \sum_{\{\mu,\nu\}\in A} |\mu\rangle\langle\mu|(\hat{h}^\alpha - \hat{h}^\beta)|\nu\rangle\langle\nu| \tag{22}$$

This definition of the on-site potentials leads to an expression for J that is consistent with the one given in ref 31. It should be noted that this definition of the on-site potentials is not unique (which is discussed in the section 7 of the Supporting Information). By inserting eq 22 into eq 20, we get

$$\begin{aligned} J^{\text{unit}}_{\text{Green}}(\text{F}) = -\frac{1}{4} Tr[& \sum_{i\in\text{occ},j} \sum_{\substack{\{\mu,\nu\}\in A \\ \{\mu',\nu'\}\in B}} |\mu\rangle\langle\mu|(\hat{h}^\alpha - \hat{h}^\beta)|\nu\rangle\langle\nu| \\ & \phi_i^\alpha\rangle\langle\phi_i^\alpha|\mu'\rangle\langle\mu'|(\hat{h}^\alpha - \hat{h}^\beta)|\nu'\rangle\langle\nu'|\phi_j^\beta\rangle \\ & \langle\phi_j^\beta|\frac{1}{\epsilon_i^\alpha - \epsilon_j^\beta} + \sum_{j\in\text{occ},i} \sum_{\substack{\{\mu,\nu\}\in A \\ \{\mu',\nu'\}\in B}} |\mu\rangle\langle\mu|(\hat{h}^\alpha - \hat{h}^\beta) \\ & |\nu\rangle\langle\nu|\phi_i^\alpha\rangle\langle\phi_i^\alpha|\mu'\rangle\langle\mu'|(\hat{h}^\alpha - \hat{h}^\beta)|\nu'\rangle\langle\nu'|\phi_j^\beta\rangle \\ & \langle\phi_j^\beta|\frac{1}{\epsilon_j^\beta - \epsilon_i^\alpha}] \end{aligned} \tag{23}$$

Evaluating the trace and exploiting that the basis functions are orthonormal, we obtain

$$\begin{aligned} J^{\text{unit}}_{\text{Green}}(\text{F}) = -\frac{1}{4}[& \sum_{i\in\text{occ},j} \sum_{\substack{\{\mu,\nu\}\in A \\ \{\mu',\nu'\}\in B}} \langle\mu|(\hat{h}^\alpha - \hat{h}^\beta)|\nu\rangle\langle\nu|\phi_i^\alpha\rangle\langle\phi_i^\alpha| \\ & \mu'\rangle\langle\mu'|(\hat{h}^\alpha - \hat{h}^\beta)|\nu'\rangle\langle\nu'|\phi_j^\beta\rangle\langle\phi_j^\beta|\mu\rangle\frac{1}{\epsilon_i^\alpha - \epsilon_j^\beta} \\ & + \sum_{j\in\text{occ},i} \sum_{\substack{\{\mu,\nu\}\in A \\ \{\mu',\nu'\}\in B}} \langle\mu|(\hat{h}^\alpha - \hat{h}^\beta)|\nu\rangle\langle\nu|\phi_i^\alpha\rangle\langle\phi_i^\alpha|\mu'\rangle \\ & \langle\mu'|(\hat{h}^\alpha - \hat{h}^\beta)|\nu'\rangle\langle\nu'|\phi_j^\beta\rangle\langle\phi_j^\beta|\mu\rangle\frac{1}{\epsilon_j^\beta - \epsilon_i^\alpha}] \end{aligned} \tag{24}$$

The matrix elements $\langle\mu|(\hat{h}^\alpha - \hat{h}^\beta)|\nu\rangle$ can be rewritten as the difference between elements of the α and β Fock matrices $F^\alpha_{\mu\nu} - F^\beta_{\mu\nu}$ in a Löwdin (or symmetrically orthogonalized) basis, resulting in

$$\begin{aligned} J^{\text{unit}}_{\text{Green}}(\text{F}) = -\frac{1}{4}[& \sum_{i\in\text{occ},j} \sum_{\substack{\{\mu,\nu\}\in A \\ \{\mu',\nu'\}\in B}} C^\alpha_{\nu i}(F^\alpha_{\mu\nu} - F^\beta_{\mu\nu})C^{\beta*}_{\mu j}C^{\alpha*}_{\mu' i} \\ & (F^\alpha_{\mu'\nu'} - F^\beta_{\mu'\nu'})C^\beta_{\nu' j}\frac{1}{\epsilon_i^\alpha - \epsilon_j^\beta} \\ & + \sum_{j\in\text{occ},i} \sum_{\substack{\{\mu,\nu\}\in A \\ \{\mu',\nu'\}\in B}} C^\alpha_{\nu i}(F^\alpha_{\mu\nu} - F^\beta_{\mu\nu}) \\ & C^{\beta*}_{\mu j}C^{\alpha*}_{\mu' i}(F^\alpha_{\mu'\nu'} - F^\beta_{\mu'\nu'})C^\beta_{\nu' j}\frac{1}{\epsilon_j^\beta - \epsilon_i^\alpha}] \end{aligned} \tag{25}$$

with the MO coefficients $C^\sigma_{\nu i} = \langle\nu|\phi_i^\sigma\rangle$.

The sum over occupied molecular orbitals can be reformulated by employing Fermi functions at 0 K

$$\lim_{T\to 0} f_i^\alpha(T) = \lim_{T\to 0} \frac{1}{\exp^{\epsilon_i^\alpha - \mu/kT} + 1} = \begin{cases} 1 & \forall \quad \epsilon_i^\alpha < \mu \\ 0 & \forall \quad \epsilon_i^\alpha > \mu \end{cases} \tag{26}$$

Assuming real molecular orbitals and exploiting the symmetry of the Fock matrix, we get the final expression for the coupling constant (compare a related expression in ref 51):

$$\begin{aligned} J^{\text{unit}}_{\text{Green}}(\text{F}) = \frac{1}{4}[& \sum_{i,j} \sum_{\{\mu,\nu\}\in A} \sum_{\{\mu',\nu'\}\in B} \frac{f_i^\alpha - f_j^\beta}{\epsilon_j^\beta - \epsilon_i^\alpha} C^\alpha_{\mu i}(F^\alpha_{\mu\nu} - F^\beta_{\mu\nu}) \\ & C^\beta_{\nu j}C^\alpha_{\mu' i}(F^\alpha_{\mu'\nu'} - F^\beta_{\mu'\nu'})C^\beta_{\nu' j}] \end{aligned} \tag{27}$$

This expression will be used in the following.

The final equations are, in general, applicable to the ferromagnetically coupled (high-spin) state and to the BS determinant modeling the antiferromagnetically coupled state. Because of the assumed cosine dependence of the energy on relative spin orientations, the sign of eq 7 and eqs 11−28 changes when applied to the BS determinant:

$$J^{\text{unit}}_{\text{Green}}(\text{AF}) = -J^{\text{unit}}_{\text{Green}}(\text{F}) \tag{28}$$

As pointed out later, this relation is not fulfilled in practice. While the Green's-function approach when applied to a ferromagnetically coupled determinant ($J^{\text{unit}}_{\text{Green}}$ (F)) is qualitatively consistent with Noodleman's Broken-Symmetry approach, it gives inconsistent results and at times wildly varying results when applied to a Broken-Symmetry determinant modeling the antiferromagnetically coupled state (see section 6 and section 7).

For completeness, it should also be noted that we use the term "(Noodleman's) Broken-Symmetry approach" to denote the approach described in section 2.2. Since the Green's function approach can in principle also be applied to a Broken-Symmetry determinant, a more exact expression for the Broken-Symmetry approach in this context would be "energy-difference approach." To be consistent with the quantum chemistry literature, we will stick with the term "Broken-Symmetry approach" in the following.

4. COMPUTATIONAL METHODOLOGY

Molecular structures were obtained by defining the structural parameters (small model systems in section 5 and dicopper complexes in section 8) or by structure optimizations (all following sections) using TURBOMOLE 6.0[52] with the BP86 exchange−correlation functional[53,54] in the resolution-of-the-identity (RI) approximation[55,56] and Ahlrich's triple-ζ def-TZVP

DOI: 10.1021/acs.jctc.5b00349
J. Chem. Theory Comput. 2015, 11, 5651−5664

basis set[57,58] with polarization functions on all atoms. For the 1,8-bis(vanadocenyl)naphthalene complex, we addionally have used the empirical dispersion correction of Grimme,[59] denoted with "-D" in the structure optimizations. The convergence criteria for the structure optimizations were set to a gradient norm below 10^{-4} au, and for the self-consistent-field (SCF) algorithm, to an energy change below 10^{-7} au.

On top of these structures, we have performed single-point calculations with GAUSSIAN09[60] using the following exchange–correlation functionals: BP86,[53,54] PBE,[61−64] TPSSH,[61−63,65,66] B3LYP,[53,61,62,67−69] and LC-ωPBE.[70−72] The convergence criteria for the SCF algorithm were set to an energy change below 10^{-6} au in all single-point calculations.

Coupling constants according to eq 28 were calculated with a new module JGREEN in our in-house program ARTAIOS,[42] which postprocesses output from electronic structure codes which can write out the relevant matrices and coefficients. For comparison with coupling constants from the BS approach, the obtained $J^{\mathrm{unit}}_{\mathrm{Green}}$ was divided by the lengths of the local spin vectors according to eq 4, where we assumed ideal local spins (e.g., one-half per formally unpaired electron).

The non-collinear DFT calculations were performed as single-point calculations on the optimized high-spin structures employing the OPENMX 3.7.1[30] program, the PBE functional, an energy cutoff-energy value of 250 Ry, pseudopotentials for the decription of the core electrons as implemented in OPENMX, and an electronic temperature of 300 K in all calculations. The following atomic basis functions have been used in the non-collinear calculations: H (H7.0-s2p1), C (C7.0-s2p2d1), O (O7.0-s2p2d1), Mn (Mn10.0-s3p2d2), S (S7.0-s2p2d1), N (N7.0-s2p2d1), Co (Co10.0H-s3p2d2), and V (V10.0-s3p2d2)). The Lagrangian multipliers of the penalty functions were increased step by step until a penalty energy lower than 10^{-6} au was achieved. Scalar relativistic effects were considered because of the j-dependence of the pseudopotentials.

5. PARAMETER STUDY ON SMALL SYSTEMS

For examination of our implementation of Lichtenstein's Green's function approach, we first have studied the hydrogen dimer as a very simple model of direct exchange spin coupling, and the H–He–H model system for superexchange coupling, where the spin-carrying hydrogen atoms are bridged by a helium atom which is modeling a closed-shell bridge.

5.1. Dihydrogen Molecule. In this section, we compare the magnetic exchange coupling in the dihydrogen molecule as a function of the distance between the hydrogen atoms (Figure 1). In this system, each hydrogen carries one unpaired electron, resulting in a triplet high-spin and a singlet low-spin state. To investigate the influence of the basis set and the exchange–correlation functional, we have applied the pure functional BP86, the hybrid functional B3LYP, and basis sets of different size (SVP, TZVP, and QZVP). The local spins are plus−minus one-half for all parameters and distances (see Figure S1 in the Supporting Information).

J_{Green}(F) (red curve) is close to the $J_{\mathrm{BS,unprojected}}$ expression (green curve), while the absolute J_{Green}(AF) values (black curve) are larger and in all cases in between the projected (blue curve) and the unprojected Noodleman expression. For B3LYP and for larger basis sets, J_{Green}(AF) is closer to $J_{\mathrm{BS,projected}}$ than for BP86 and for smaller basis sets. For all of the parameters used, we find the same qualitative trends with a very similar order of the different J values, but quantitatively we find deviations up to a factor of 4.

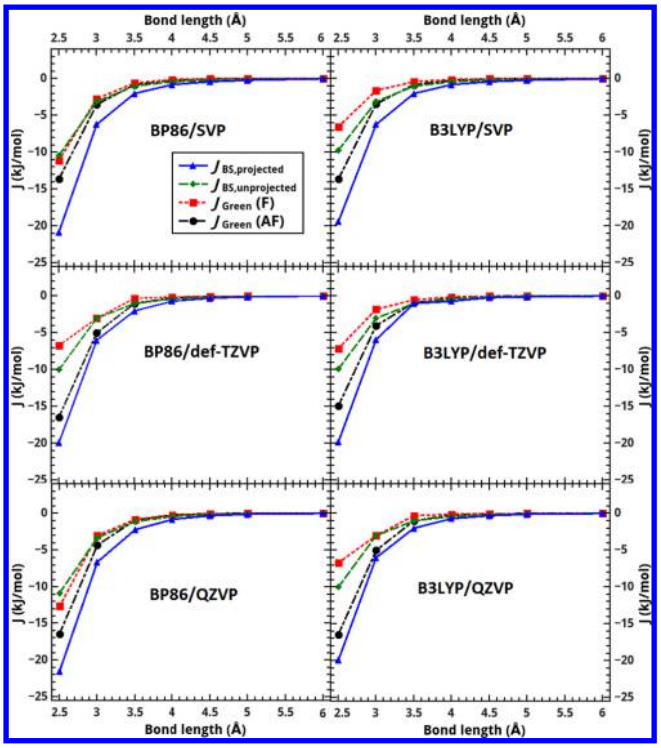

Figure 1. Magnetic coupling constants obtained from the Green's function approach J_{Green}(F)/J_{Green}(AF) and the magnetic coupling constants calculated within the projected and unprojected BS formalism for the BP86 and the B3LYP functional and different basis sets for the dihydrogen molecule at different bond lengths.

5.2. H–He–H Model System. In contrast to the direct spin interactions in the dihydrogen molecule, the H–He–H model system exhibits superexchange via a bridging closed-shell helium atom. As for the dihydrogen molecule, we obtain a triplet high-spin state approximated by a BS determinant. To evaluate the influence of the strength of the coupling on the performance of the Green's function approach, we have considered three different H–He bond distances (1.25, 1.625, and 2.0 Å). For these calculations, we applied two different basis sets (def-TZVP and QZVP) and four exchange-correlation functionals, since the electronic structure (e.g., the local spins) is expected to show a larger dependence on the applied exchange-correlation functional compared with the dihydrogen molecule. The cosine behavior of the energy as a function of the angle θ between the two local spins was confirmed for these systems by noncollinear DFT calculations with the PBE functional (see section 8 in the Supporting Information). The changes in the magnetic exchange coupling constants according to an increase in the basis set size turned out to be very small, so that only the results obtained with def-TZVP are discussed here and the QZVP results are given in the Supporting Information. In Figure 2, the local spins of the hydrogen atoms (left column) and the calculated magnetic exchange coupling constants (right column) obtained for the three different bond lengths are given. The local spins on the helium bridge are not shown since they were zero for all distances.

The local spin analysis reveals that for the smallest bond length (1.25 Å) the magnitudes are about 0.1 au smaller in the high-spin state than for the BS solution, while the differences for the other two distances are rather small. This influences the calculated magnetic exchange coupling constants, since the Green's-function approach assumes a spin rotation without any changes

DOI: 10.1021/acs.jctc.5b00349
J. Chem. Theory Comput. 2015, 11, 5651−5664

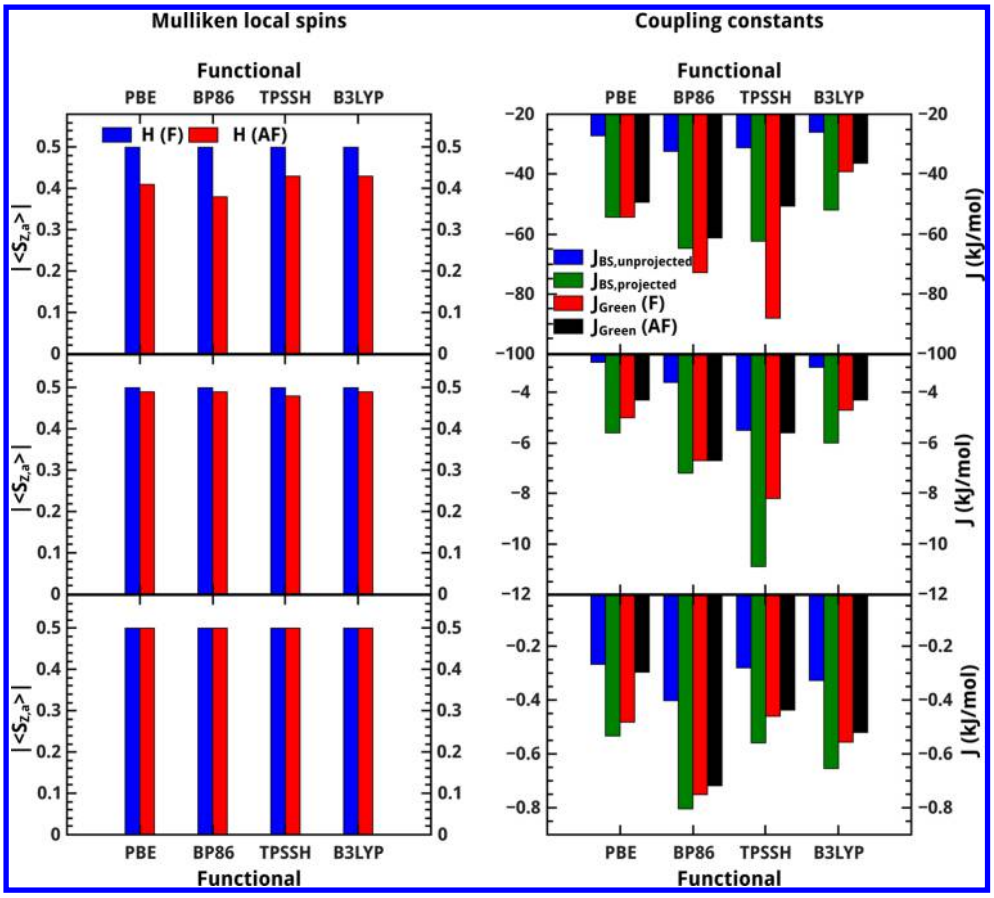

Figure 2. Local spins of the hydrogen atoms (left column), the magnetic exchange coupling constants (right column) calculated within the Green's-function approach $J_{Green}(F)/J_{Green}(AF)$, and the magnetic coupling constants calculated for the H−He−H model system within the projected and unprojected BS formalism for the BP86 and the B3LYP functional at three different H−He bond lengths, 1.25 Å (top), 1.625 Å (middle), and 2.0 Å (bottom).

in the spins' magnitudes. So we find for a bond length of 1.25 Å that $J_{Green}(F)$ (red bars) is higher than $J_{BS,projected}$ (green bars) for all applied exchange-correlation functionals except for B3LYP, where we find $J_{Green}(F)$ in between $J_{BS,projected}$ and $J_{BS,unprojected}$ (blue bars). But in all cases, the $J_{Green}(AF)$ (black bars) are smaller than the $J_{Green}(F)$ values. For the higher bond distances where the spin remains the same independent of the spin configuration, we find that the $J_{Green}(F)$ values are always between the values obtained from the unprojected and the projected formula. The $J_{Green}(AF)$ values still remain the same relative to the BS values. Although we find in general good qualitative agreement between both methods, no general scaling factor can be given here. Additionally, one should always keep in mind the sensitivity of the Green's-function approach to changes in the spins' magnitudes, violating the picture of rotating spins.

6. LARGER SYSTEMS WITH LOCALIZED SPINS

In this section, we describe a number of dinuclear complexes with different electronic configurations to see if the Green's function approach is able to describe more complicated electronic structures. The complexes chosen for these studies are shown in Figure 3. The structures were optimized in their high-spin and low-spin states (approximated by BS solutions), and coupling constants were calculated for both spin-state structures. The para-bridged dimethylene radical was only optimized in the high-spin state, and we additionally increased the bond length between the methylene groups and the phenyl bridge up to 1.8 Å to be able to obtain an open-shell BS determinant. Again non-collinear DFT calculations with PBE (Supporting Information) on the high-spin structures gave proof of a cosine behavior of the energy as a function of the angle θ between the two local spins for all systems studied in this section, only for the para-C_8H_8 diradical, small deviations are found around 90°. The coupling constants are in good agreement with those obtained with GAUSSIAN09, which is an important prequisite for comparing the results (see section 8 in the Supporting Information).

Depending on the spin state in which the structure optimization was carried out, we get a further stabilization of this spin-states if single-point calculations are carried out on this structure for both spin states.[73,74] The main purpose of this section lies again on the agreement between both methods, but we also want to see how strong the magnetic exchange coupling constants are affected by the choice of the structure. This is especially important for the Green's-function approach, since it is applied on one spin state and, therefore, no structural relaxation effects can be taken into account.

Because the Green's-function approach needs the definition of the spin centers, we have performed a Mulliken local spin analysis for each compound to investigate if the spin remains on the spin centers or if it is reduced, meaning a higher degree of spin delocalization onto adjacent atoms, which could falsify the obtained magnetic coupling constants for the Green's-function approach. The local spin analysis revealed that the spins are very close to the ideal spins given in Figure 3 and are therefore not

DOI: 10.1021/acs.jctc.5b00349
J. Chem. Theory Comput. 2015, 11, 5651−5664

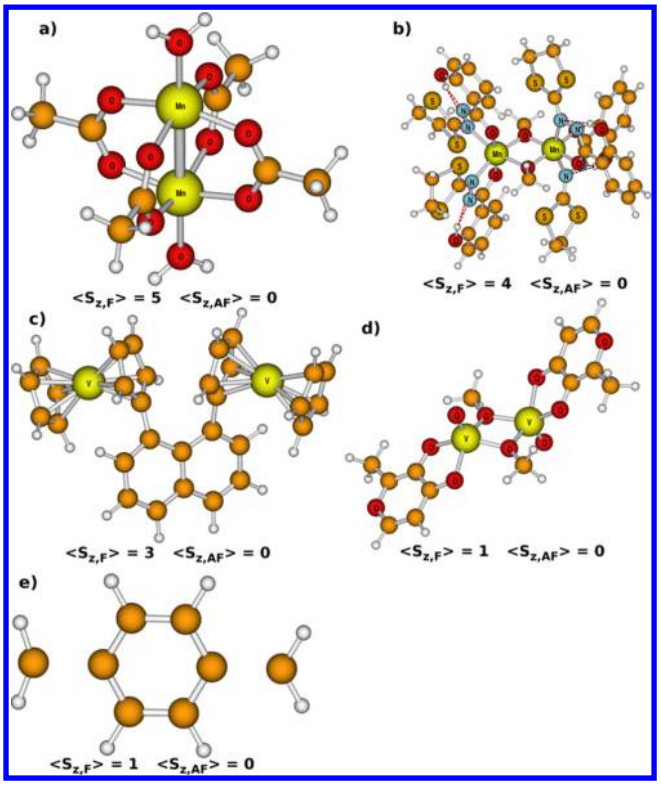

Figure 3. Structures and ideal $\hat{S}_z$ expectation values in both spin states for systems with localized spins optimized in the high-spin state (BP86/def-TZVP; (c) optimized with Grimme's dispersion correction). (a) $[Mn_2(Ac)_4(H_2O)_2]$, (b) $[Mn_2(\mu\text{-}OMe)_2(HL)_4]$; H_2L = (2-salicyloylhydrazono-1,3-dithiolane), (c) $[V_2(\eta^5\text{-}Cp)_2(\mu\text{-}\eta^5\text{-}1,8\text{-}DCN)$] 1,8-DCN = 1,8-dicyclopentadienylnaphthalene dianion; Cp = Cyclopentadienyl anion, (d) $[V_2(\mu\text{-}O\text{-}Me)_2(O)_2(ma)_2]$, ma = maltato, (e) para-C_8H_8 (C−C bond length between benzene and methylene group was artificially elongated to 1.8 Å).

discussed explicitly, but they are given in the Supporting Information.

The magnetic exchange coupling constants calculated with different exchange-correlation functionals are given in Figure 4 for the structures optimized in the ferromagnetically coupled and the antiferromagnetically coupled BS determinant. As expected, the structures with an antiferromagnetic ground state optimized for the BS spin-configurations are coupled more strongly antiferromagnetic than the systems optimized in the high-spin state. Also the magnetic exchange coupling constants calculated for the ferromagnetically coupled $[Mn_2(\mu\text{-}OMe)_2(HL)_4]$ complex are stronger for the structure optimized in the high-spin state than for the BS structure. The coupling constants obtained within the BS approach with LC-ω-PBE for this system are strongly overestimated for both spin-state structures compared to the results produced by the other functionals. The same overestimation is also found for the single-point calculations performed on the BS structure of the $[V_2(\mu\text{-}O\text{-}Me)_2(O)_2(ma)_2]$ complex characterized by Sun and co-workers[75] and described with non-collinear DFT by Peralta and Barone.[33] The $J_{Green}(F)$ values are in the order of the other functionals; therefore the problem may arise from the BS determinant in those cases. In all cases, the same qualitative trends are found for the BS formalism and for the Green's-function method applied to the high-spin state ($J_{Green}(F)$, red). Only the results obtained from the Green's-function approach applied to the BS determinants ($J_{Green}(AF)$, black) give magnetic exchange coupling constants which deviate in most cases quantitatively (e.g., for the bis-vanadocenyl complex, where the $J_{Green}(AF)$ values are between −0.12 kJ/mol and −0.25 kJ/mol, which in combination with the very small $J_{Green}(F)$ and J_{BS} values leads to a large relative deviation) or even qualitatively (e.g., for $[Mn_2(\mu\text{-}OMe)_2(HL)_4]$) from those obtained from the BS approach. It is interesting that for the $[V_2(\mu\text{-}O\text{-}Me)_2(O)_2(ma)_2]$ complex, which was studied in ref 33, $J_{Green}(F)$ and $J_{Green}(AF)$ are in good agreement with each other. Because the non-collinear calculations did not show any deviations from a cosine potential energy surface for the other complexes studied in this section, the problems might be related to the BS determinant itself. For nearly all systems, we can find that the coupling constants $J_{Green}(F)$ for the pure functionals (BP86 and PBE) are rather comparable with the $J_{BS,projected}$ values (green bars), while coupling constants obtained for the hybrid functionals as TPSSH and B3LYP are comparable to the unprojected values $J_{BS,unprojected}(F)$. The same is true for LC-ω-PBE for which the exchange coupling from the Green's-function approach is always much weaker than the coupling predicted with the BS approach. A more detailed discussion of these relations is given at the end of the next section (Figure 9).

7. LARGER SYSTEMS WITH DELOCALIZED SPINS

In this part of the work, we focus on systems with a higher degree of spin delocalization. This is interesting since it is questionable if the metal centers are still a good choice for the definition of magnetic sites if the spin is transferred to adjacent atoms. Therefore, we chose two different complexes, a $[Cu_2(\mu\text{-}Ac)_4(H_2O)_2]$ complex and a $[Co_2(\eta^5\text{-}Cp)_2(\mu\text{-}\eta^5\text{-}1,8\text{-}DCN)]$ complex, both having formally one electron per metal center. Furthermore, we investigate a meta-substituted dimethylene-benzene diradical (see Figure 5) with a triplet high-spin and singlet low-spin state. All compounds were optimized in both spin states. For the high-spin structures, non-collinear DFT calculations were performed, but due to convergence problems, no data were obtained for the $[Cu_2(\mu\text{-}Ac)_4(H_2O)_2]$ complex. For the $[Co_2(\eta\text{-}Cp)_2(\mu\text{-}\eta^5\text{-}1,8\text{-}DCN)]$ complex, the angular dependence shows a cosine shape, while for the meta-C_8H_8, the deviations are very strong (see section 8 in the Supporting Information).

We performed a Mulliken local spin analysis to get information about the degree of spin delocalization in the molecules studied here. Since the deviations between the spin centers are small, the local spins in Figure 6 are given for one spin center only (the values for both centers are given in Figure S4 in the Supporting Information). We found that the degree of spin delocalization increases from $[Co_2(\eta^5\text{-}Cp)_2(\mu\text{-}\eta^5\text{-}1,8\text{-}DCN)]$, where the spin on the Co(II) centers is roughly 0.4 au, to the $[Cu_2(Ac)_4(H_2O)_2]$ complex were the spin is only 0.3 au on each copper atom. We can further see that the spin on the methylene carbon atoms in the meta-C_8H_8 diradical seems to be strongly localized, but there are significant negative and positive spin densities on the carbon atoms of the bridging benzene ring in the high-spin state, while none can be found for the BS solution (see Figure 7 and section 4.4 in the Supporting Information). For the other molecules in this section, the magnitude of the local spins remains nearly independent of the spin state (see sections 4.1−4.3 in the Supporting Information). It can further be seen that the spin on the metal centers is slightly lower for the BS determinants than for the high-spin states, but for the hybrid functionals and LC-ωPBE the spins on the centers are very similar. The only

DOI: 10.1021/acs.jctc.5b00349
J. Chem. Theory Comput. 2015, 11, 5651−5664

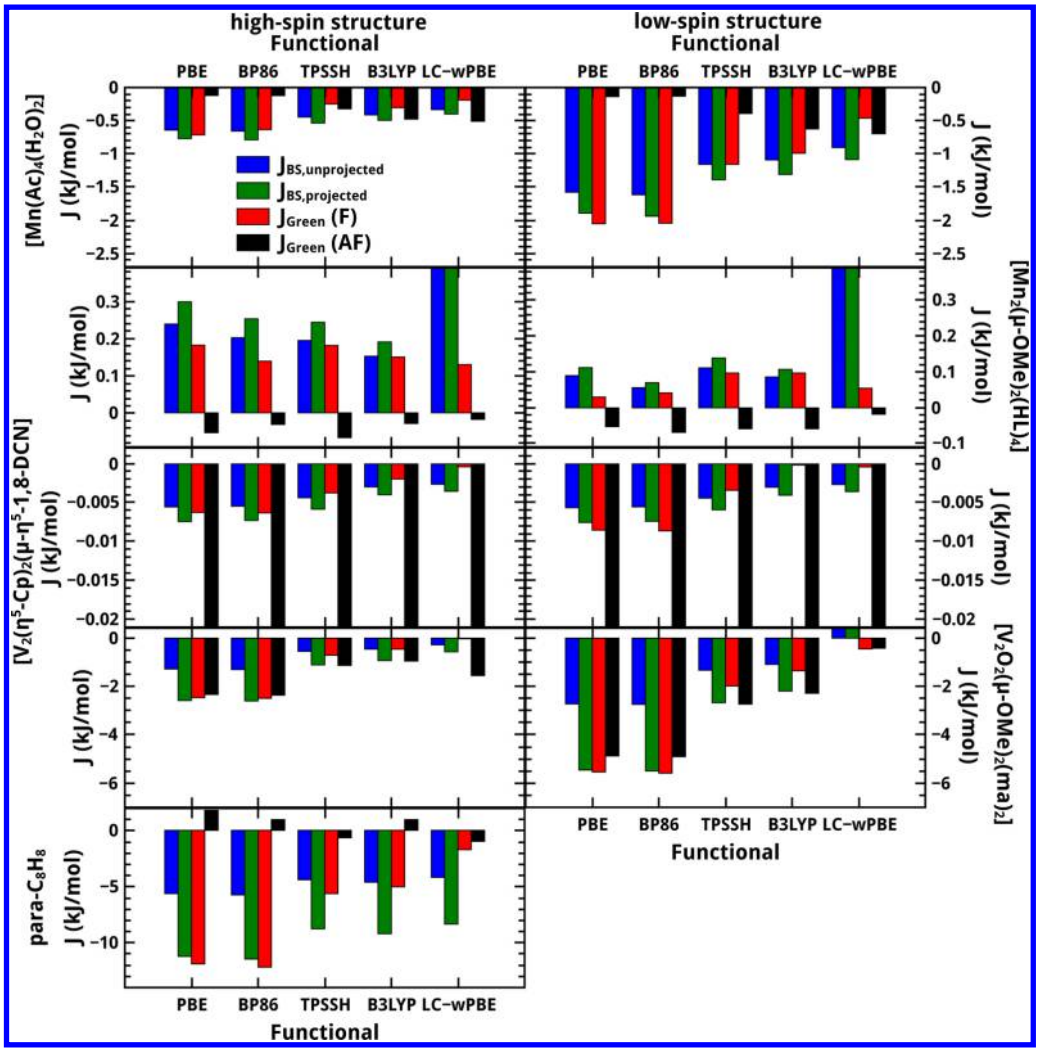

Figure 4. Magnetic exchange coupling constants obtained with different functionals for the compounds given in Figure 3 and different spin-state structures. LC-ωPBE BS values for $[Mn_2(\mu\text{-OMe})_2(HL)_4]$ (high-spin and BS structure) and $[V_2(\mu\text{-O-Me})_2(O)_2(ma)_2]$ (BS structure) are larger than the displayed range. Basis set: def-TZVP.

exception is again meta-C_8H_8, where the local spin is slightly larger in the BS determinant.

The calculated magnetic coupling constants given in Figure 8 reveal that for the transition-metal complexes the coupling constants are in very good agreement with those obtained by the BS approach. For the dinuclear copper complex, we observe the same trends as for the transition complexes discussed in the previous section. As in the section before, we find that all $J_{Green}(F)$ values obtained for the 1,8-bis(cobaltocenyl)-naphthalene complex with pure functionals are comparable with those obtained for the projected Noodleman expression, while we find a better agreement between $J_{Green}(F)$ and the values of the unprojected formula.

For the 1,8-bis(cobaltocenyl)naphthalene complex, we find qualitatively different coupling constants depending on the spin state in which the structure was optimized. So we find ferromagnetic coupling for the high-spin structure, while we find antiferromagnetic coupling for the optimized structure of the BS solution. Even the coupling constants obtained from the BS approach by using the optimized spin-state structures (Supporting Information, Table S4) are ambiguous because the pure functionals, the B3LYP hybrid functional and LC-ωPBE, give ferromagnetic coupling, while TPSSH predicts antiferromagnetic coupling. Experimental studies on this system performed by Pagels and co-workers[76] agree with the TPSSH functional and reveal an antiferromagnetically coupled ground state. To quantify the structural changes from one spin-state structure to the other, we investigated the several structural parameters for the 1,8-bis(cobaltocenyl)naphthalene complex and the 1,8-bis(vanadocenyl)naphthalene from the previous section, where the changes in the magnetic coupling constants were much smaller. We also investigated structural parameters in the $[Cu_2(Ac)_4(H_2O)_2]$, where the coupling constants changed strongly. The structural parameters are not discussed explicitly here but are given in the Supporting Information (section 4). However, this comparison revealed that the structural changes in the copper complex and the biscobaltocenyl complex are larger than in the vanadocenyl complex, where nearly all parameters are constant independent of the spin-state stucture. We find that the deviations in the magnetic exchange coupling constants correlate with the extent of the structural changes from one spin state to another. This shows how crucial the effect of structural relaxation on the magnetic exchange coupling can be. It may be that molecules for which different resonance structures can be written (for the 1,8-bis(cobaltocenyl)naphthalene complex, a closed-shell Lewis structure featuring two Co(I) centers could be

DOI: 10.1021/acs.jctc.5b00349
J. Chem. Theory Comput. 2015, 11, 5651−5664

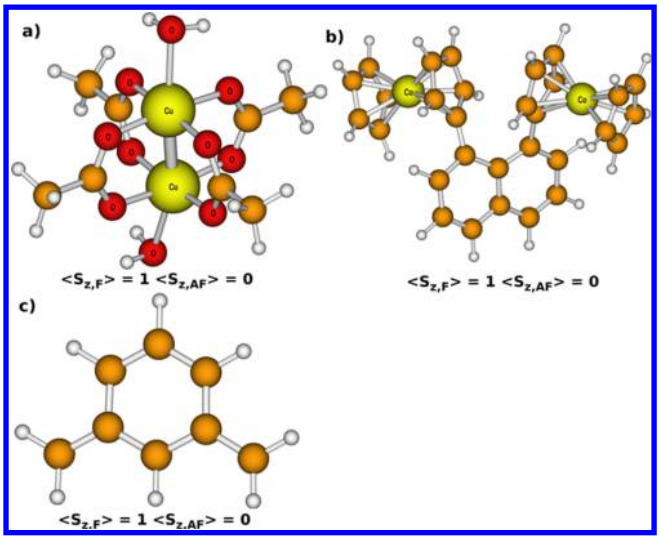

Figure 5. Structures and ideal $\hat{S}_z$ expectation values in both spin states for systems with delocalized spins optimized in the high-spin state (BP86/def-TZVP). (a) Tetra-μ-acetato-diaqua-dicopper(II), $[Cu_2(Ac)_4(H_2O)_2]$. (b) 1,8-Bis(cobaltocenyl)naphthalene, $[Co_2(\eta^5\text{-}Cp)_2(\mu\text{-}\eta^5\text{-}1,8\text{-}DCN)]$, 1,8-DCN = 1,8-dicyclopentadienylnaphthalene dianion, Cp = Cyclopentadienyl anion. (c) Meta-dimethylenebenzene, meta-C_8H_8. (d) para-dimethylenebenzene, meta-C_8H_8.

formulated) are particularly susceptible to such effects, but this would have to be checked in future work.

For the structure optimized in the BS solution, we can observe for LC-ωPBE that the coupling constants obtained from the BS

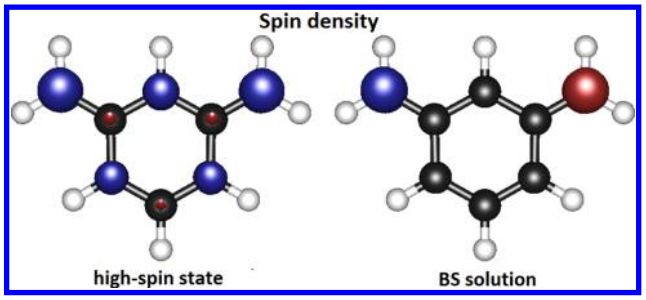

Figure 7. Spin density in the meta-C_8H_8 diradical for the high-spin state and the BS solution (BP86/def-TZVP). Single-point calculations on top of the optimized high-spin structure.

approach are strongly ferromagnetic, which is not in agreement with all other functionals and the experimental measurements.[76] Such unreliable results were also found for the ferromagnetically coupled complex in the previous section. The $J_{Green}(F)$ value is negative here but much too low, so that one could think again of problems in the description of the BS solution.

For meta-C_8H_8, we find strong quantitative deviations from the BS approach, which might be a result of the strong spin-delocalization onto the bridge. So it would be better to include the atoms on the benzene bridge, which is problematic because the magnetic sites share the same atoms on the bridge, and therefore it is not possible to split them up properly in two magnetic sites.

Although we have seen that there is no general scaling factor between the values obtained from the Green's-function approach

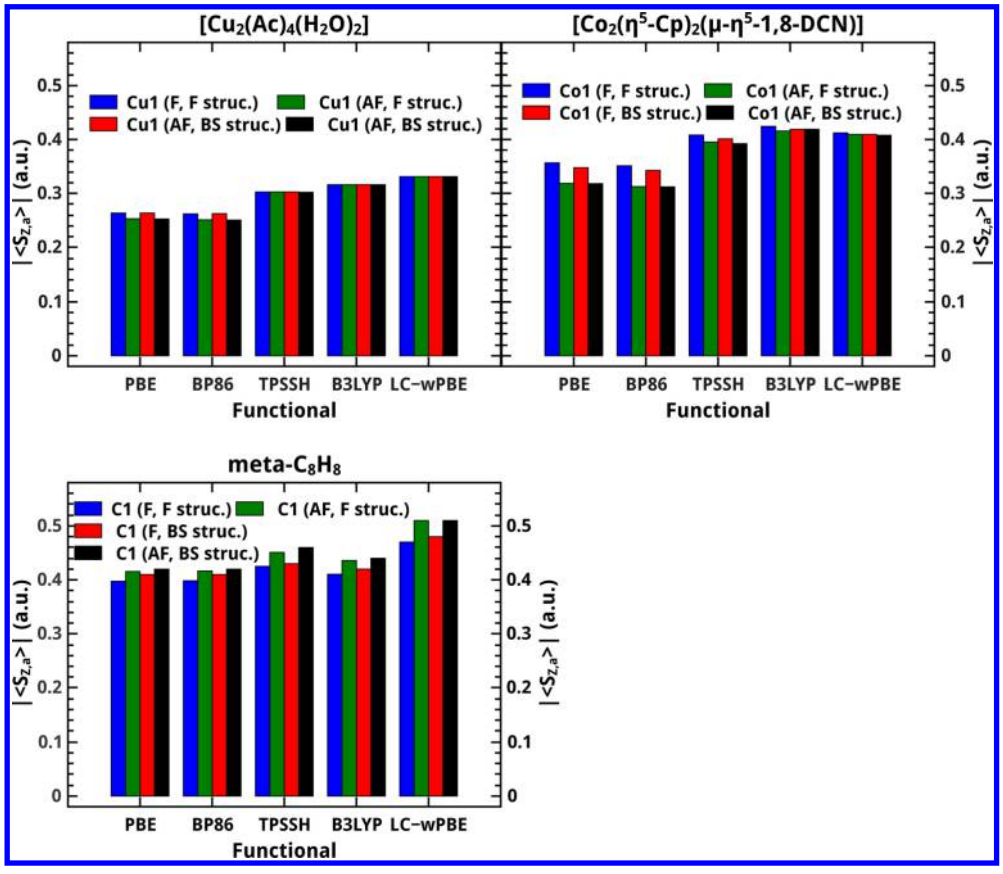

Figure 6. Mulliken local spins for the different compounds, spin states, and spin-state structures given in Figure 5 for different functionals. In all cases, only the spin of the main atom has been taken into account. Basis set: def-TZVP.

DOI: 10.1021/acs.jctc.5b00349
J. Chem. Theory Comput. 2015, 11, 5651−5664

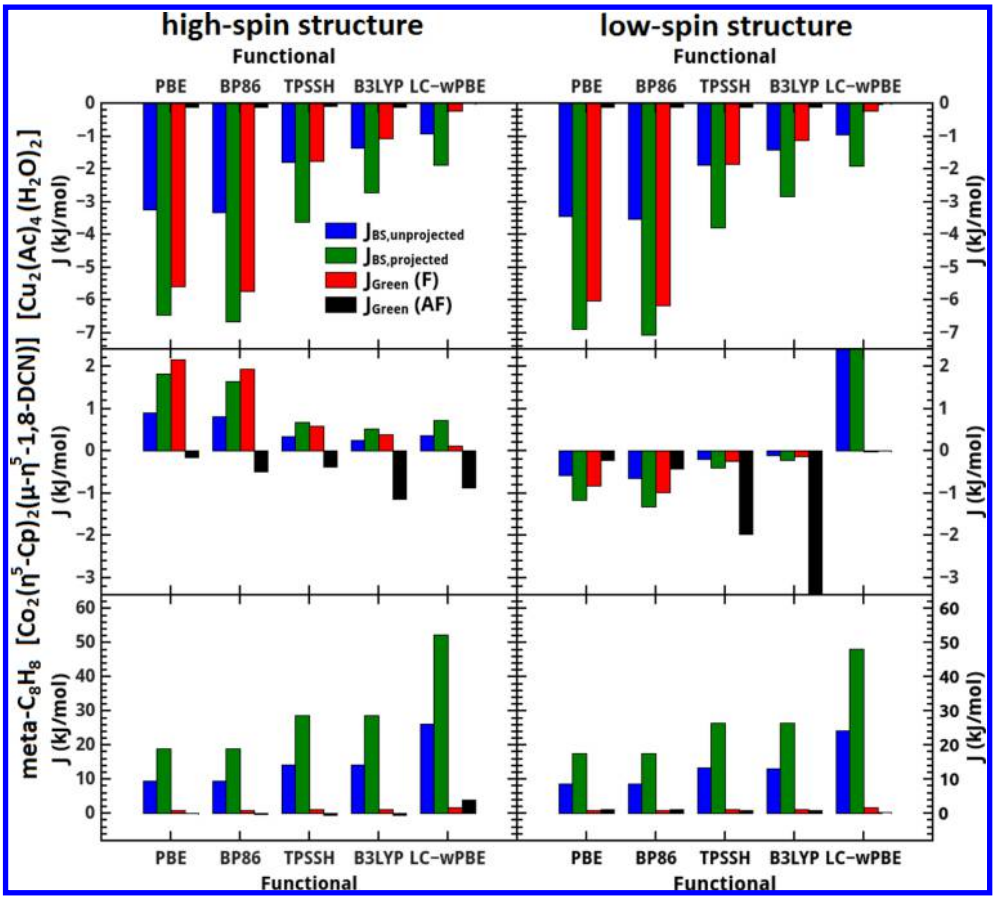

Figure 8. Magnetic coupling constants for the compounds given in Figure 5 for different spin state structures and exchange-correlation functionals. For the low-spin structure of 1,8-bis(cobaltocene)benzene, the LC-ωPBE BS values are larger than the displayed range. Basis set: def-TZVP.

and the BS formulas, we are interested in evaluating whether $J_{Green}(F)$ values are generally closer to the values obtained from the BS approach with or without spin projection ($J_{BS,projected}$ and $J_{BS,unprojected}$) for the different functionals under study here. To quantify our observations, we have calculated mean average percentage errors (MAPE) from all magnetic exchange coupling constants obtained for the compounds in this and the previous section:

$$\mathrm{MAPE}(J_{BS,projected}) = \frac{100}{n}\sum_{t=1}^{n}\left|\frac{J_{BS,projected} - J_{Green}(F)}{J_{BS,projected}}\right| \quad (29)$$

$$\mathrm{MAPE}(J_{BS,unprojected}) = \frac{100}{n}\sum_{t=1}^{n}\left|\frac{J_{BS,unprojected} - J_{Green}(F)}{J_{BS,unprojected}}\right| \quad (30)$$

MAPEs for $J_{Green}(AF)$ were not calculated since we found in most cases quantitative and qualitative deviations, and therefore these values do not seem reliable at all. The MAPEs for $J_{Green}(F)$ are given in Figure 9. The meta-C_8H_8 diradical was not considered at all due to the problems with the definition of the magnetic sites. For LC-ωPBE, the results obtained for [$Mn_2(\mu$-OMe)$_2$(HL)$_4$] (high-spin and BS structure), [$V_2(\mu$-OMe)$_2$(O)$_2$(ma)$_2$] (BS structure), and the [$Co_2(\eta^5$-Cp)$_2(\mu$-η^5-1,8-DCN)] (BS structure) were not considered due to problems with the BS values.

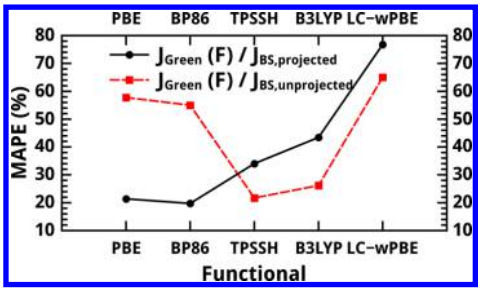

Figure 9. Mean absolute percentage errors (MAPEs) calculated according to eqs 29 and 30 for different exchange-correlation functionals considering all transition-metal complexes in this and the last section. Basis set: def-TZVP.

The MAPEs for the $J_{Green}(F)/J_{BS,projected}$ couple reveal that the values differ in only about 20% for the pure functionals as PBE and BP86, while we find MAPEs of roughly 35% for TPSSH, 43% for B3LYP, and 77% for LC-ωPBE. For the $J_{Green}(F)/J_{BS,unprojected}$ couple, we find that the MAPEs are 58% and 55% for PBE and BP86, while the MAPEs for the hybrid functionals are about 20% (TPSSH, 21%; B3LYP, 26%) and 65% for LC-ωPBE. So we can see that for pure functionals the $J_{Green}(F)$ values approach those obtained with the projected formula, while we find the opposite for the hybrid functionals and the LC-ωPBE. These results suggest a systematic dependence on the applied exchange−correlation functional and possibly on the amount of exact Hartree−Fock exchange included (but further studies would be needed for a more solid statement). In general, the performance

DOI: 10.1021/acs.jctc.5b00349
J. Chem. Theory Comput. 2015, 11, 5651−5664

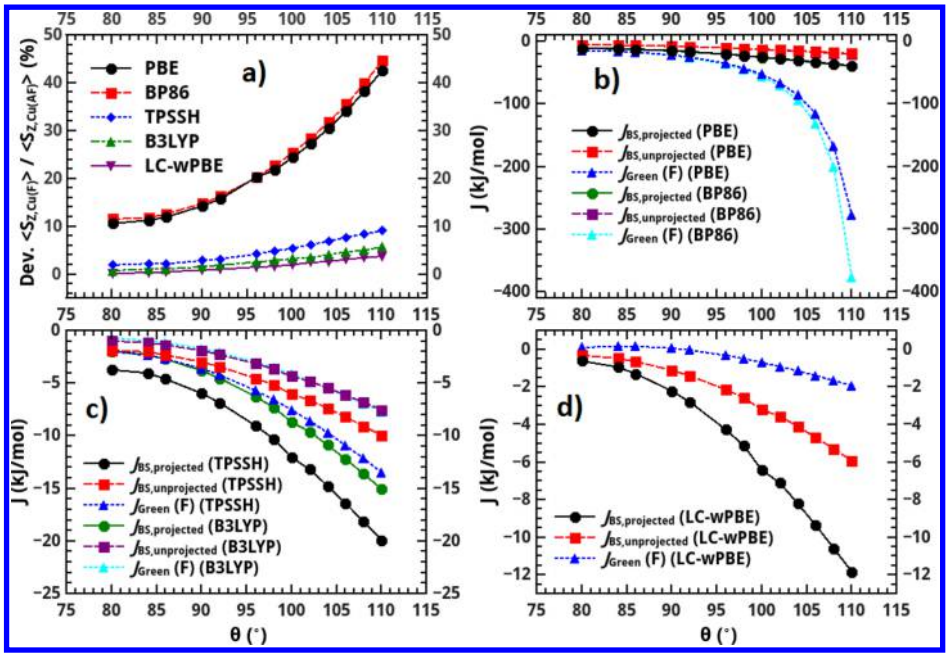

Figure 10. (a) Deviations of the local spins on the copper(II) centers between the high-spin state and the BS solution. (b–d) Calculated magnetic exchange coupling constants obtained with different functionals as a function of Cu–O–Cu angle θ. Basis set: def-TZVP.

of LC-ωPBE in combination with the Green's-function approach deviates more from the Broken-Symmetry results than for all other functionals, since the exchange coupling is underestimated for most of the systems considered here.

8. BOND-ANGLE DEPENDENCE OF EXCHANGE COUPLING CONSTANTS IN SYSTEMS WITH DELOCALIZED SPINS

The Green's-function method reproduced the trends obtained for the H_2 and the H–He–H molecules by the BS approach well, and therefore we are interested to see if such structural correlations are that well described in transition-metal complexes. It is known from the literature[1,77−80] that the magnetic exchange coupling in ligand-bridged dinuclear complexes strongly depends on the metal–ligand–metal angles. Therefore, we evaluate the dependence of the magnetic exchange coupling constants on the Cu–O–Cu angle θ in a $[Cu_2(\mu\text{-}OH)_2Cl_4]^{2-}$ complex. This complex was already studied in further depth by Hoffmann and Hay,[1] and it was observed increasing antiferromagnetic coupling with increasing Cu–O–Cu angle. Angles between 80° and 110° were investigated by varying the angle in steps of 2° (single-point calculations for 82°, 88°, and 94° did not converge). All other structural parameters were fixed to the values given in ref 1 and are given in the methodology. The local spin analysis (see Supporting Information) reveals that the spin is highly delocalized onto the ligands, so that only local spins between 0.23 and 0.3 au remain on the copper atoms depending on the angle and the applied functional. In general, the local spins on the copper(II) centers increase slightly with increasing angle and also with increasing Hartree–Fock exchange. The LC-ωPBE functional gives the strongest localization on the copper(II) centers.

Following the HDvV Hamiltonian only spin rotation is taken into account; therefore we plotted the deviations of the local spins on the copper atoms in the high-spin state and the BS solution in percent (Figure 10). The deviations between both spin states are increased with increasing angle θ for the pure functionals as BP86 and PBE, while for TPSSH, B3LYP, and LC-ω-PBE, the deviations are significantly smaller. These deviations in the local spins on the copper(II) centers have a drastic effect of the coupling constants calculated within the Green's-function approach, so that the antiferromagnetic exchange coupling is strongly overestimated by PBE and BP86 at higher Cu–O–Cu angles. For TPSSH and B3LYP where the deviations between the local spins in both spin configurations are rather small, the trends obtained by the BS approach are well reproduced by the Green's-function approach. Only the coupling constants calculated with LC-ω-PBE are underestimated compared with the BS approach, which was found for all complexes discussed in this study.

9. CONCLUSION

In this work, we discuss an alternative method to the Broken-Symmetry approach for the evaluation of magnetic exchange coupling constants which is based on Green's functions and which has been well established in the solid state community.[28] The advantage of this approach is that the coupling constant can be calculated from the high-spin state, circumventing the calculation of the Broken-Symmetry determinant. In contrast to the conceptionally similar method of Peralta and co-workers,[34] which solves the coupled-perturbed Kohn–Sham equations iteratively, the coupling constant in the Green's-function method can be obtained in one step, at the price of neglecting orbital relaxation. We implemented this approach in a postprocessing tool JGreen for quantum chemistry program packages, evaluated coupling constants for several compounds, and compared these values with values obtained from spin-state energy differences within the Broken-Symmetry approach.

For the simple model systems, the dihydrogen and the H–He–H molecules, we found that the Green's-function approach gives the same qualitative trends as for the BS approach. While in the case of the dihydrogen molecule $J_{Green}(F)$ is comparable with $J_{BS,unprojected}$ and $J_{Green}(AF)$ is comparable with $J_{BS,projected}$, the opposite is found for H–He–H. Therefore, we cannot give a general scaling factor for comparing the BS and the Green's-

DOI: 10.1021/acs.jctc.5b00349
J. Chem. Theory Comput. 2015, 11, 5651−5664

function method. The study on H−He−H further revealed that the Green's-function method is sensitive to changes in the magnitude of spins from one spin state to the other.

In the BS approach, the structures of both spin states can be optimized separately, while the Green's-function method is applied to one spin-state only, and no structural relaxation effects can be taken into account. Therefore, we investigated several transition-metal complexes and the influence of the spin-state structures on the evaluated magnetic exchange coupling constants. For the coupling constants, we found the expected shift to stronger antiferromagnetic coupling for the structures optimized using a BS determinant for both methods. In the case of the 1,8-bis(cobaltocene)complex, we found that both methods give a ferromagnetically coupled ground state for the high-spin structure and an antiferromagnetically coupled ground state for the Broken-Symmetry structure. This demonstrates that in some cases structural relaxation effects are crucial to obtaining qualitative agreement with the reference data and additionally reveals a potential pitfall of the Green's-function approach. Except for some results obtained with the LC-ω-PBE functionals, where the coupling constants can deviate strongly compared with all other functionals, we find a good qualitative agreement between J_{Green}(F) and the BS energy-difference formalism, while the J_{Green}(AF) values are in many cases in qualitative disagreement with the BS approach. Non-collinear DFT calculations did not show any deviations from the cosine behavior of the HDvV Hamiltonian. Therefore, the problems seems to be related to the BS determinant itself. From these observations, we can conclude that the Green's-function method should only be applied on the high-spin state and not on the BS determinant.

We could further show that the increasing delocalization of the spin density in those systems does not drastically affect the calculated magnetic exchange coupling constants as long the spins' magnitudes remain the same for both spin states. A problematic issue is molecules as the meta-dimethylenebenzene where two magnetic sites share atoms on the bridge, so that a proper definition of the two magnetic sites is no longer possible. Additionally, the non-collinear DFT calculations reveal strong deviations from a cosine behavior of the energy as a function of the angle between the two local spins. The mean average percentage errors (MAPEs) that the coupling constants obtained for the pure functionals (PBE and BP86) are rather comparable with the $J_{BS,projected}$ values, while the coupling constants obtained from the hybrid functionals (as TPSSH and B3LYP) are rather comparable with the $J_{BS,projected}$ values.

We also investigated the bond-angle dependence of the magnetic exchange coupling constants in a dinuclear copper(II) complex, to see if the Green's-function method is able to reproduce the structure−property correlations obtained from the BS approach. We could see that although only half of the spin remains on the copper(II) centers, the trends predicted with the Green's-function approach are in very good agreement for TPSSH and B3LYP, while we find for BP86 and PBE strong deviations between both methods due to the deviations in the local spins in the high-spin state and the BS solution, which violates the picture of local spins of fixed length assumed in the Heisenberg−Dirac−Van Vleck Hamiltonian.

Applied to the high-spin state, the Green's-function method gives qualitative agreement with the results obtained with the BS approach and therefore constitutes a good alternative method with reduced computational cost. The drawbacks are that no orbital relaxation and structural relaxation effects are taken into account. For future work, it appears worthwhile to focus more on the problems concerning the description of magnetic exchange coupling constants in organic radicals. Since magnetic exchange coupling constants can be decomposed in pairs of α- and β-spin orbitals within the Green's-function method, it would also be interesting to test its applicability as a tool for the analysis of exchange pathways.[81−84] This may be relevant for the design of new molecular magnetic systems or materials.

■ ASSOCIATED CONTENT

Supporting Information

The Supporting Information is available free of charge on the ACS Publications website at DOI: 10.1021/acs.jctc.5b00349.

Local spins, results with a larger basis set for the H−He−H system, magnetic coupling constants calculated with the broken-symmetry approach from the optimized spin-state structures of $[Co_2(\eta^5\text{-Cp})_2(\mu\text{-}\eta^5\text{-1,8-DCN})]$, structural parameters of complexes optimized in different spin states, an alternative formulation of J_{Green}, the resulting coupling constants for all systems under study, the non-collinear DFT results obtained with OpenMX, cartesian coordinates and total energies of all complexes and diradicals (PDF)

■ AUTHOR INFORMATION

Corresponding Author

*Phone: +49-40-42838-6934. E-mail: carmen.herrmann@chemie.uni-hamburg.de.

Notes

The authors declare no competing financial interest.

■ ACKNOWLEDGMENTS

We thank the Collaborative Research Center (Sonderforschungsbereich) SFB 668 (projects B17 and A3). T.S. and C.H. further acknowledge the Fonds der Chemischen Industrie for funding and the regional computing center (RRZ) for computational resources.

■ REFERENCES

(1) Hay, P. J.; Thibeault, J. C.; Hoffmann, R. *J. Am. Chem. Soc.* **1975**, *97*, 4884−4889.
(2) Layfield, R. A. *Organometallics* **2014**, *33*, 1084−1099.
(3) Lineberger, W. C.; Borden, W. T. *Phys. Chem. Chem. Phys.* **2011**, *13*, 11792−11813.
(4) Anderson, P. W. *Phys. Rev.* **1950**, *79*, 350−356.
(5) Anderson, P. W. *Phys. Rev.* **1959**, *115*, 2−13.
(6) Lee, J.; Lee, E.; Kim, S.; Bang, G. S.; Shultz, D. A.; Schmidt, R. D.; Forbes, M. D. E.; Lee, H. *Angew. Chem., Int. Ed.* **2011**, *50*, 4414−4418.
(7) Pronschinske, A.; Chen, Y.; Lewis, G. F.; Shultz, D. A.; Calzolari, A.; Buongiorno Nardelli, M.; Dougherty, D. B. *Nano Lett.* **2013**, *13*, 1429−1434.
(8) Herrmann, C.; Yu, L.; Reiher, M. *J. Comput. Chem.* **2006**, *27*, 1223−1239.
(9) Fillol, J. L.; Condola, Z.; Garcia-Bosch, I.; Gomez, L.; Pla, J. J.; Costas, M. *Nat. Chem.* **2011**, *3*, 807−813.
(10) Biswas, S.; Dutta, A.; Dolai, M.; Bhowmik, I.; Rouzieres, M.; Lee, H. M.; Clerac, R.; Ali, M. *Eur. J. Inorg. Chem.* **2013**, *2013*, 4922−4930.
(11) Bruijnincx, P.; Buurmans, I.; Huang, Y.; Juhasz, G.; Viciano-Chumillas, M.; Quesada, M.; Reedjik, J.; Lutz, M.; Spek, A.; Münck, E.; Bominaar, E. L.; Gebbink, R. K. *Inorg. Chem.* **2011**, *50*, 9243−9255.
(12) Herrmann, C.; Elmisz, J. *Chem. Commun.* **2013**, *49*, 10435.
(13) Proppe, J.; Herrmann, C. *J. Comput. Chem.* **2015**, *36*, 201−209.
(14) Kirk, M. L.; Shultz, D. A.; Depperman, E. C.; Brannen, C. L. *J. Am. Chem. Soc.* **2007**, *129*, 1937−1943.
(15) Feng, D.; Wang, C.; Cheng, W.; Li, G.; Tian, S.; Liao, F.; Ming, X.; Lin, J. *Solid State Sci.* **2003**, *11*, 845−851.

DOI: 10.1021/acs.jctc.5b00349
J. Chem. Theory Comput. 2015, 11, 5651−5664

(16) El Fallah, M. S. E.; Vicente, R.; Escuer, A.; Badyine, F.; Solans, X.; Font-Bardia, M. *Inorg. Chim. Acta* **2008**, *361*, 4065−4069.
(17) Trtica, S.; Prosenc, M. H.; Schmidt, M.; Heck, J.; Albrecht, O.; Goerlitz, D.; Reuter, F.; Rentschler, E. *Inorg. Chem.* **2010**, *49*, 1667−1673.
(18) Abedi, A.; Khavasi, H. R.; Amani, V.; Safari, N. *Dalton Trans.* **2011**, *40*, 6877−6885.
(19) Mautner, F. A.; Navarro, M.; Speed, S.; El Fallah, M. S.; Font-Bardia, M.; Vicente, R. *Polyhedron* **2013**, *52*, 866−871.
(20) Gobeze, W. A.; Milway, V. A.; Chilton, N. F.; Moubaraki, B.; Murray, K. S.; Brooker, S. *Eur. J. Inorg. Chem.* **2013**, *2013*, 4485−4498.
(21) Parr, R. G.; Yang, W. *Density-Functional Theory of Atoms and Molecules*; Oxford University Press: New York, 1989.
(22) Noodleman, L. *J. Chem. Phys.* **1981**, *74*, 5737−5743.
(23) Cramer, C. J.; Truhlar, D. G. *Phys. Chem. Chem. Phys.* **2009**, *11*, 10757−10816.
(24) Chlopek, K.; Muresan, N.; Neese, F.; Wieghardt, K. *Chem. - Eur. J.* **2007**, *13*, 8390−8403.
(25) Pantazis, D.; Krewald, V.; Orio, M.; Neese, F. *Dalton Trans.* **2010**, *39*, 4959−4967.
(26) Bhave, D. P.; Han, W.-G.; Pazicni, S.; Penner-Hahn, J. E.; Carroll, K. S.; Noodleman, L. *Inorg. Chem.* **2011**, *50*, 6610−6625.
(27) Vogiatzis, K. D.; Klopper, W.; Mavrandonakis, A.; Fink, K. *ChemPhysChem* **2011**, *12*, 3307−3319.
(28) Liechtenstein, A. I.; Katsnelson, M. I.; Gubanov, V. *J. Phys. F: Met. Phys.* **1984**, *14*, L125−L128.
(29) Liechtenstein, A. I.; Katsnelson, M. I.; Gubanov, V. A. *J. Magn. Magn. Mater.* **1987**, *67*, 65−74.
(30) Ozaki, T.; Kino, H.; Yu, J.; Han, M. J.; Ohfuchi, M.; Ishii, F.; Sawada, K.; Kubota, Y.; Ohwaki, T.; Weng, H.; Toyoda, M.; Kawai, H.; Okuno, Y.; Perez, R.; Bell, P.; Duy, T.; Xiao, Y.; Ito, A.; Terakura, K. OpenMx: Open source package for Material EXplorer. http://www.openmx-square.org/.
(31) Han, M.; Ozaki, T.; Yu, J. *Phys. Rev. B: Condens. Matter Mater. Phys.* **2004**, *70*, 184421.
(32) Brunhold, T. C.; Gamelin, D. R.; Solomon, E. I. *J. Am. Chem. Soc.* **2000**, *122*, 8511−8523.
(33) Peralta, J. E.; Barone, V. *J. Chem. Phys.* **2008**, *129*, 194107.
(34) Philips, J. J.; Peralta, J. E. *J. Chem. Phys.* **2013**, *138*, 174115.
(35) Bornemann, S.; Slpr, O.; Mankovsky, S.; Polesya, S.; Staunton, J.; Wurth, W.; Minar, H. E. A. J. *Phys. Rev. B: Condens. Matter Mater. Phys.* **2012**, *86*, 104436.
(36) Ebert, H.; Ködderitzsch, D.; Minar, J. *Rep. Prog. Phys.* **2011**, *74*, 096501.
(37) Han, M. J.; Ozaki, T.; Yu, J. *Phys. Rev. B: Condens. Matter Mater. Phys.* **2007**, *75*, 060404.
(38) Yildirim, T. *Phys. C* **2009**, *469*, 425−441.
(39) Polesya, S.; Mankovsky, S.; Sipr, O.; Meindl, W.; Strunk, C.; Ebert, H. *Phys. Rev. B: Condens. Matter Mater. Phys.* **2010**, *82*, 214409.
(40) Purdum, H.; Montano, P. A.; Shenoy, G. K.; Morrison, T. *Phys. Rev. B: Condens. Matter Mater. Phys.* **1982**, *25*, 4412−4417.
(41) Clark, A. E.; Davidson, E. R. *Int. J. Quantum Chem.* **2003**, *93*, 384−394.
(42) Herrmann, C.; Groß, L.; Steenbock, T.; Solomon, G. C. ARTAIOS − a transport code for postprocessing quantum chemical electronic structure calculations. 2008−2014.
(43) Anderson, P. W. *Solid State Phys.* **1963**, *14*, 99.
(44) Antropov, V.; Katsnelson, M.; Harmon, B.; van Schilfgaarde, M.; Kusnezov, D. *Phys. Rev. B: Condens. Matter Mater. Phys.* **1996**, *54*, 1019−1023.
(45) Pople, J. A.; Gill, P. M. W.; Handy, N. C. *Int. J. Quantum Chem.* **1995**, *56*, 303−305.
(46) Jacob, C.; Reiher, M. *Int. J. Quantum Chem.* **2012**, *112*, 3661−3684.
(47) Löwdin, P.-O. *J. Chem. Phys.* **1950**, *18*, 365.
(48) Mulliken, R. S. *J. Chem. Phys.* **1955**, *23*, 1833.
(49) Herrmann, C.; Reiher, M.; Hess, B. A. *J. Chem. Phys.* **2005**, *122*, 034102.
(50) Szabo, A.; Ostlund, N. S. *Modern Quantum Chemistry*; Dover Publications Inc.: Mineola, NY, 1996; p 231.
(51) Antropov, V.; Katsnelson, M.; Liechtenstein, A. *Phys. B* **1997**, *237*−*238*, 336−340.
(52) *TURBOMOLE*, V6.0; University of Karlsruhe and Forschungszentrum Karlsruhe GmbH: Karlsruhe, Germany, 1989−2007; TURBOMOLE GmbH: Karlsruhe, Germany, 2007. Available from http://www.turbomole.com.
(53) Becke, A. *Phys. Rev. A: At., Mol., Opt. Phys.* **1988**, *38*, 3098.
(54) Perdew, J. P. *Phys. Rev. B: Condens. Matter Mater. Phys.* **1986**, *33*, 8822−8824.
(55) Eichkorn, K.; Treutler, O.; Ohm, H.; Haser, M.; Ahlrichs, R. *Chem. Phys. Lett.* **1995**, *240*, 283−289.
(56) Eichkorn, K.; Weigend, F.; Treutler, O.; Ahlrichs, R. *Theor. Chem. Acc.* **1997**, *97*, 119−124.
(57) Schäfer, A.; Horn, H.; Ahlrichs, R. *J. Chem. Phys.* **1992**, *97*, 2571−2577.
(58) Schäfer, A.; Huber, C.; Ahlrichs, R. *J. Chem. Phys.* **1994**, *100*, 5829−5835.
(59) Antony, J.; Grimme, S. *Phys. Chem. Chem. Phys.* **2006**, *8*, 5287−5293.
(60) Frisch, M. J.; Trucks, G. W.; Schlegel, H. B.; Scuseria, G. E.; Robb, M. A.; Cheeseman, J. R.; Scalmani, G.; Barone, V.; Mennucci, B.; Petersson, G. A.; Nakatsuji, H.; Caricato, M.; Li, X.; Hratchian, H. P.; Izmaylov, A. F.; Bloino, J.; Zheng, G.; Sonnenberg, J. L.; Hada, M.; Ehara, M.; Toyota, K.; Fukuda, R.; Hasegawa, J.; Ishida, M.; Nakajima, T.; Honda, Y.; Kitao, O.; Nakai, H.; Vreven, T.; Montgomery, J. A., Jr.; Peralta, J. E.; Ogliaro, F.; Bearpark, M.; Heyd, J. J.; Brothers, E.; Kudin, K. N.; Staroverov, V. N.; Kobayashi, R.; Normand, J.; Raghavachari, K.; Rendell, A.; Burant, J. C.; Iyengar, S. S.; Tomasi, J.; Cossi, M.; Rega, N.; Millam, N. J.; Klene, M.; Knox, J. E.; Cross, J. B.; Bakken, V.; Adamo, C.; Jaramillo, J.; Gomperts, R.; Stratmann, R. E.; Yazyev, O.; Austin, A. J.; Cammi, R.; Pomelli, C.; Ochterski, J. W.; Martin, R. L.; Morokuma, K.; Zakrzewski, V. G.; Voth, G. A.; Salvador, P.; Dannenberg, J. J.; Dapprich, S.; Daniels, A. D.; Farkas, Ö.; Foresman, J. B.; Ortiz, J. V.; Cioslowski, J.; Fox, D. J. *Gaussian 09*, Revision A.1; Gaussian, Inc.: Wallingford, CT, 2009.
(61) Dirac, P. *Proc. R. Soc. London, Ser. A* **1929**, *123*, 714.
(62) Slater, J. *Phys. Rev.* **1951**, *81*, 385.
(63) Perdew, J.; Wang, Y. *Phys. Rev. B: Condens. Matter Mater. Phys.* **1992**, *45*, 1200.
(64) Perdew, J.; Burke, K.; Ernzerhof, M. *Phys. Rev. Lett.* **1996**, *77*, 3865−3868.
(65) Tao, J.; Perdew, J.; Staroverov, V.; Scuseria, G. *Phys. Rev. Lett.* **2003**, *91*, 146401.
(66) Staroverov, V. N.; Scuseria, G. E.; Tao, J.; Perdew, J. P. *J. Chem. Phys.* **2003**, *119*, 12129−12136.
(67) Vosko, S.; Wilk, L.; Nusair, M. *Can. J. Phys.* **1980**, *58*, 1200.
(68) Lee, C.; Yang, W.; Parr, R. *Phys. Rev. B: Condens. Matter Mater. Phys.* **1988**, *37*, 785.
(69) Becke, A. *J. Chem. Phys.* **1993**, *98*, 5648−5652.
(70) Vydrov, O.; Scuseria, G. *J. Chem. Phys.* **2006**, *125*, 234109.
(71) Vydrov, O.; Heyd, J.; Krukau, A.; Scuseria, G. *J. Chem. Phys.* **2006**, *125*, 074106.
(72) Vydrov, O.; Scuseria, G.; Perdew, J. *J. Chem. Phys.* **2007**, *126*, 154109.
(73) Bovi, D.; Guidoni, L. *J. Chem. Phys.* **2012**, *137*, 114107.
(74) Melo, J. I.; Phillips, J. J.; Peralta, J. E. *Chem. Phys. Lett.* **2013**, *557*, 110−113.
(75) Sun, Y.; Melchior, M.; Summers, D. A.; Thompson, R. C.; Rettig, S. J.; Orvig, C. *Inorg. Chem.* **1998**, *37*, 3119−3121.
(76) Pagels, N.; Albrecht, O.; Görlitz, D.; Rogachev, A.; Prosenc, M.; Heck, J. *Chem. - Eur. J.* **2011**, *17*, 4166−4176.
(77) Groß, L.; Steenbock, T.; Herrmann, C. *Mol. Phys.* **2013**, *111*, 1482−1491.
(78) Crawford, W.; Richardson, H.; Wasson, J.; Hodgson, D.; Hatfield, W. *Inorg. Chem.* **1976**, *15*, 2107−2110.
(79) Glerup, J.; Hodgson, D.; Petersen, E. *Acta Chem. Scand.* **1983**, *A37*, 161−164.

DOI: 10.1021/acs.jctc.5b00349
J. Chem. Theory Comput. 2015, 11, 5651−5664

(80) Mukherjee, R.; Stack, T.; Holm, R. *J. Am. Chem. Soc.* **1988**, *110*, 1850−1861.
(81) Le Guennic, B.; Ferré, N. *Curr. Inorg. Chem.* **2014**, *3*, 235.
(82) Pantazis, D.; Krewald, V.; Orio, M.; Neese, F. *Dalton Trans.* **2010**, *39*, 4959−4967.
(83) Brunhold, T. C.; Gamelin, D. R.; Solomon, E. I. *J. Am. Chem. Soc.* **2000**, *122*, 8511−8523.
(84) Coulaud, E.; Malrieu, J.-P.; Guihéry, N.; Ferré, N. *J. Chem. Theory Comput.* **2013**, *9*, 3429.

DOI: 10.1021/acs.jctc.5b00349
J. Chem. Theory Comput. 2015, 11, 5651−5664